

General Disclaimer

One or more of the Following Statements may affect this Document

- This document has been reproduced from the best copy furnished by the organizational source. It is being released in the interest of making available as much information as possible.
- This document may contain data, which exceeds the sheet parameters. It was furnished in this condition by the organizational source and is the best copy available.
- This document may contain tone-on-tone or color graphs, charts and/or pictures, which have been reproduced in black and white.
- This document is paginated as submitted by the original source.
- Portions of this document are not fully legible due to the historical nature of some of the material. However, it is the best reproduction available from the original submission.

**FREE-SURFACE PHENOMENA
UNDER LOW- AND ZERO-GRAVITY CONDITIONS**

(NASA-CR-175885) FREE-SURFACE PHENOMENA
UNDER LOW- AND ZERO-GRAVITY CONDITIONS
Final Technical Report (Stanford Univ.) 8 p
HC A02/MF A01 CSCI 22A

N85-27922

Unclas
G3/12 21423

**Final Technical Report
NASA Grant NAG 3-557
June 1, 1984 to March 31, 1985**

**Lambertus Hesselink
Principal Investigator**

**Stanford University
Stanford, California 94305**

June 1985



1. SUMMARY

This report summarizes the new work that has been done on the free surface experiment using a liquid doped with a fluorescent dye under sheet illumination. The work includes the selection of a CCD camera for use during the design stages of the experiment as well as a preliminary demonstration of this technique in the production of a contour map of a liquid-liquid interface with better than 0.1 mm resolution.

2. DETECTOR SELECTION

Several solid state cameras were considered. They include the RCA and Pulnix CCD cameras, as well as a GE CID (charge injection device) camera. We have limited ourselves to solid-state cameras because they exhibit no blooming effects. However, when used in conjunction with our Vicom digital image processor, they all display a regular vertical striped pattern associated with the difference in clock cycles of the camera and the Vicom. Since the Vicom is to be used for the development of the necessary processing algorithms, this background noise problem was a source of delay. For the work presented here, the Pulnix was used because it performs the best in this respect. Nevertheless, the Pulnix images contain enough of this noise to make processing difficult. Pulnix has assured us that this noise problem will be remedied soon.

In any event, this type of noise should not exist in the final experiment design, because we plan to have the detector and the processing and storage devices run by the same clock. Without this noise, the necessary image processing is reduced essentially to a simple thresholding function, which can be done by

hardware in real time.

3. EXPERIMENTAL RESULTS

The experimental set-up is diagrammed in Figure 1. A horizontal sheet of laser light, with a waist thickness of ~ 0.1 mm., passes through a rectangular glass container holding two immiscible liquids, ethylene glycol and methyl laurate. The orientation of the laser sheet (with respect to the container) was chosen to produce easily interpreted contour lines of the known liquid interface. The orientation of the laser sheet for the actual space-based experiment will depend on the container shape and size, as well as optical constraints on the size and extent of the laser sheet. For example, a laser sheet can only maintain a thickness of 0.1 mm. for a distance of about 20 mm.. So the direction of the laser sheet should either be chosen to avoid having it pass through more than 20 mm. of liquid, or more than one laser sheet can be used to illuminate different regions of the container.

The methyl laurate is doped with a fluorescent dye (LD700, from Exciton). The container is 1 cm. by 4 cm in cross-section, but only a 1 cm by 2 cm portion of this is observed by the camera. In this configuration, one camera pixel is equivalent to about 0.05 mm, thus giving better than 0.1 mm resolution in the plane of the cross-section.

For the experiment, twenty-six cross-sections were recorded, spaced 0.1 mm apart. An example of the unprocessed image is in Figure 2a. The processing steps are summarized in Figures 2b-g. The final contour map is presented in Figure 3.

The first step of the processing was to threshold the image, where the decision level was set to be approximately one-half the maximum intensity level of the image (thresholding sets everything above the decision level equal to 1, the maximum intensity, and everything below equal to 0, the minimum intensity). The result is in Figure 2b. In this figure vertical scoring can be seen, which is the result of the camera's background noise mentioned earlier. To remove this, a low-pass filter was used on the image and a threshold operation was again performed (Figures 2c,d).

In Figure 2d (as well as in the original, Figure 2a) it is apparent that the fluorescing intensity drops off toward the left side of the image. This is due to absorption of the laser light, which is coming in from the right side. This intensity inhomogeneity can be minimized by a concentration of fluorescent dye optimized for the intensity of the laser light. For this demonstration, the concentration was not optimized. Instead, the area of observation was reduced to contain only that area which was least affected by this absorption. So the next step in processing was to box off the area of interest (Figure 2e). This allowed for higher threshold values without degradation of the contour lines. Higher threshold values generally translate into lower noise.

Threshold level also determines the effective waist thickness of the light sheet. The light sheet exhibits a gaussian intensity profile, and its waist thickness is defined as the point where the power drops to $1/e^2$ of the maximum. By setting the threshold level above the $1/e^2$ value of the maximum fluorescing power, one should obtain edges that correspond to those one would obtain if the

light sheet had a well defined thickness equal to the desired waist size. For the work presented here, the threshold level was set much higher than the $1/e^2$ level (to $\sim 1/2$ maximum), thus reducing the effective waist thickness still further.

Finally, an edge detection algorithm was used to produce the contour line at that level (Figure 2f). A composite of all the contour lines was made to produce the topographic map of Figures 2g and 3.

4. CONCLUSION

We have demonstrated that this technique can be used to produce a mapping of the interface to within 0.1 mm resolution over an area of greater than 1 cm. . With a different data sampling and storage procedure, the image processing should be reduced to a simple thresholding procedure, which can be done in hardware. This reduces the needed pixel information to one bit, with no loss of topographical information. Such a procedure can easily be implemented in hardware and performed in real time.

FIGURE 1
EXPERIMENTAL CONFIGURATION

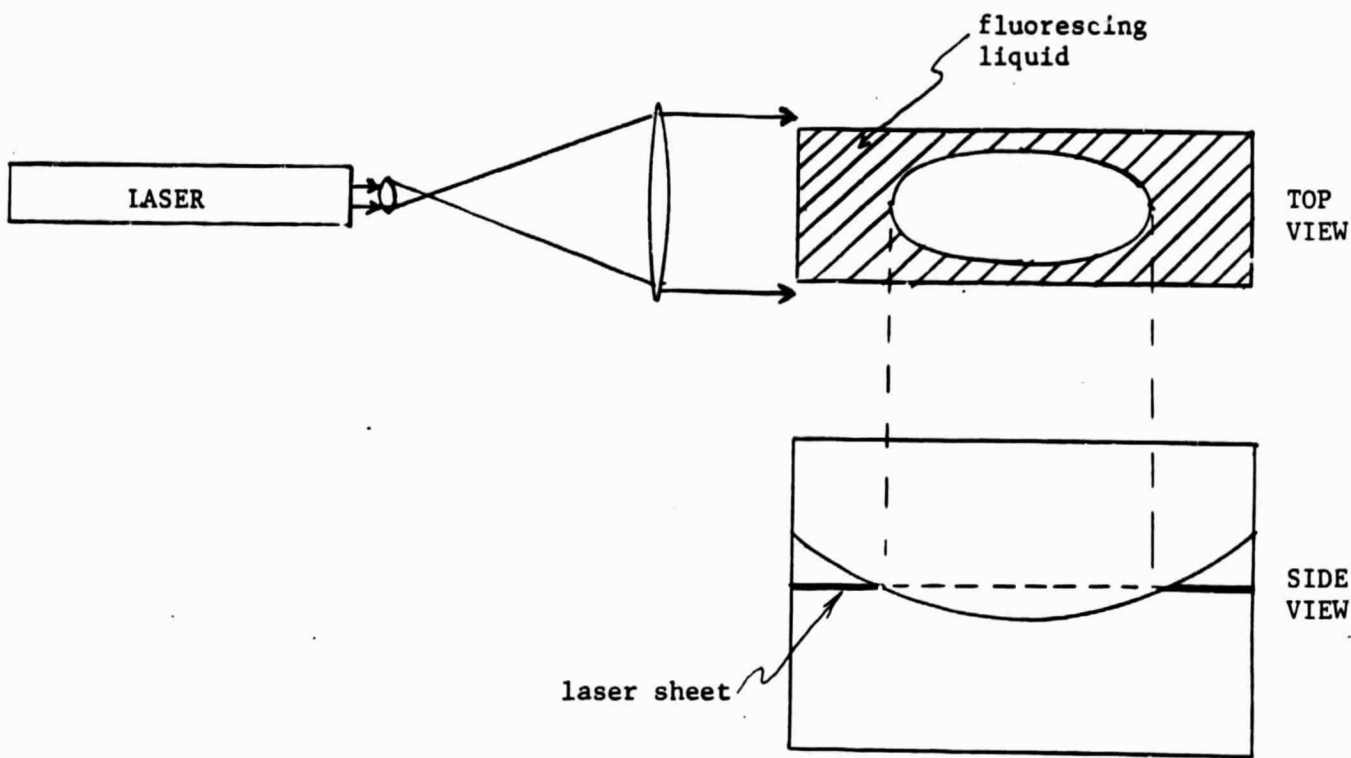
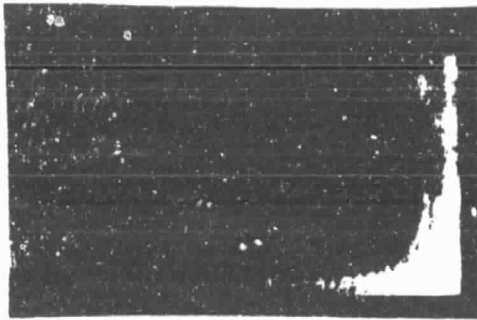
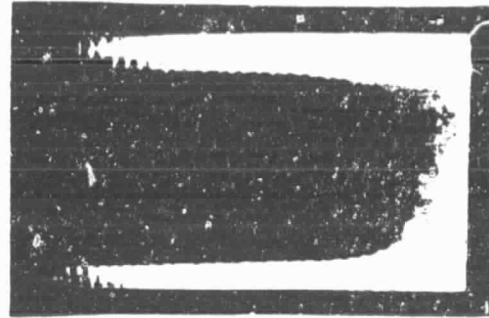


FIGURE 2
IMAGE PROCESSING

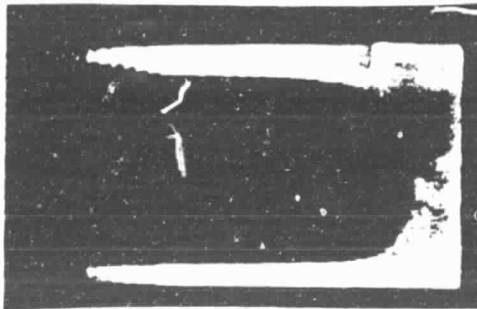
ORIGINAL PAGE IS
OF POOR QUALITY.



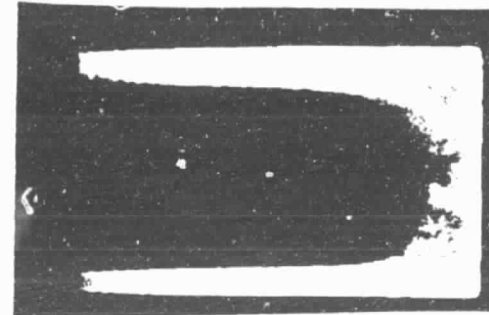
a. Original



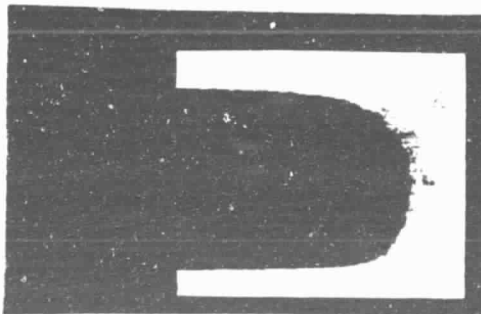
b. Threshold



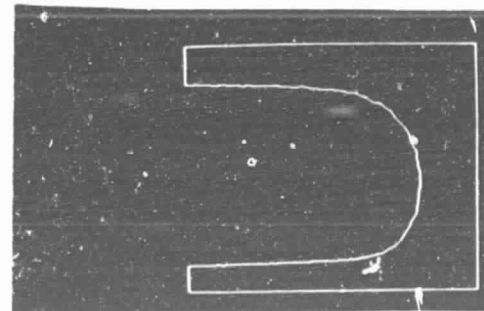
c. Low-pass filter



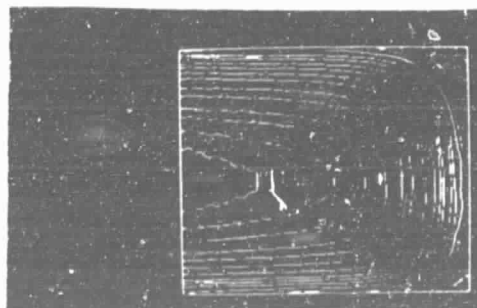
d. Threshold



e. Truncate



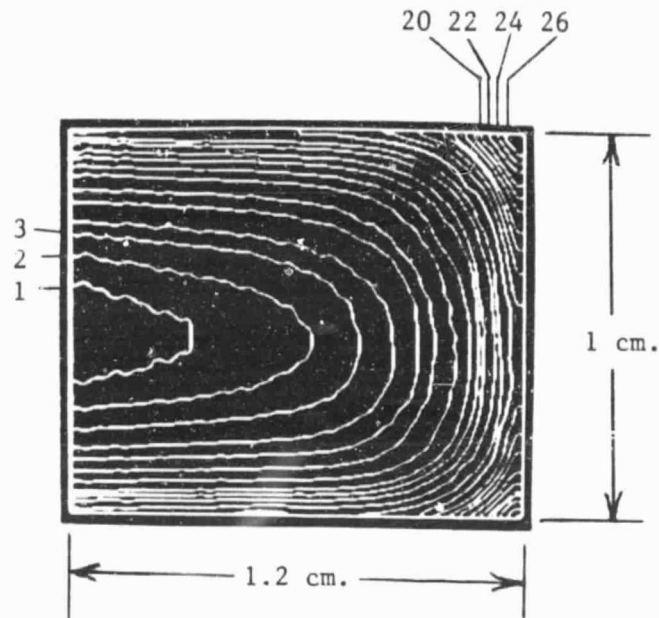
f. Edge detect



g. Composite

FIGURE 3
COMPOSITE CONTOUR MAP

ORIGINAL PAGE IS
OF POOR QUALITY



Notes

- Contour lines are numbered by increasing height.
- Spacing of contour lines is 0.1 mm.
- Contour lines 21, 23 and 25 are not included to avoid bunching.
- The top/bottom asymmetry is most likely due to the laser sheet not being exactly perpendicular to the local vertical.